UNPUBLISHED PRELIMINARY DATA

NsG-149-61

[redacted]

REDUCTION OF ERRORS IN VIBRATORY GYROSCOPES BY DOUBLE MODULATION

Richard W. Bush* George C. Newton, Jr.*

[redacted]

35209 A CR55540

ABSTRACT

Vibratory drive, vibratory output instruments for sensing angular rates, such as tuning forks, potentially offer certain advantages over conventional gyroscopes. The theoretical performance of these devices has not been realized experimentally because of zero-rate errors attributed to mass unbalance, driving force unbalance and other imperfections. By separating the driving and sensing frequencies through a process called double modulation, obtained through an additional rotation or vibration of the basic sensing element, zero rate errors may be diminished. Theoretical and experimental evidence in support of the double modulation concept is presented. A tuning fork type of instrument has been used in the initial experiments and a substantial improvement over the performance of the same instrument without double modulation has been realized.

Author

[redacted]

* Electronic Systems Laboratory, Massachusetts Institute of Technology, Cambridge 39, Massachusetts

REDUCTION OF ERRORS IN VIBRATORY GYROSCOPES BY DOUBLE MODULATION

Richard W. Bush[2] and George C. Newton, Jr.[2]

[2] (NASA Grant NsG-149-61) (NASA CR-55540)

[1964] 24 p refs

Presented at 2nd Symp. on Unconventional Inertial Sensors; for presentation at Joint Autom. Conf., Stanford U., Jun. 1964

Submitted for Publication

Conf.

INTRODUCTION

Broadly speaking, the term "vibratory gyroscope" refers to angular motion sensors that produce output signals as the result of vibratory torques or forces caused by Coriolis effects. This is in contrast to conventional gyroscopes in which the forces that give rise to output signals are steady for input angular rates that are constant. Coriolis effects in any gyroscopic instrument arise when one or more mass elements are made to move relative to the instrument frame of reference. This motion of the mass elements is called the driving motion and two general methods for achieving such motion are recognized. One is the rotary drive method where the mass elements move in circular paths at constant angular velocity. A number of ways of measuring the oscillatory Coriolis forces resulting from such motion have been devised. Although in principle the double modulation concept to be described in this paper is applicable to rotary drive instruments, the experiments conducted so far have used the second type of driving motion in which the mass elements move in an oscillatory manner along predetermined trajectories that often approximate straight lines. The discussion of this paper is limited to the second type of drive.

A large number of vibratory drive configurations are possible. Among these are: the vibrating string or wire, the tuning fork, vibratory motions in bars, plates, shells as well as acoustical vibrations in gases and liquids. Although all of these methods of imparting vibratory motion to mass elements have been considered in the literature, it is the tuning-fork that has received the greatest theoretical and experimental attention over the past 25 years. In the United States, Lyman is credited with the basic invention of the tuning-fork form of vibratory gyroscope.[1*]

The authors have chosen a tuning-fork form of instrument for their experiments because of the large literature that exists for this kind of instrument. This enables comparisons to be made with the results of other workers. However, the authors do not mean to imply that the tuning fork configuration is necessarily superior to other configurations, either as a medium for experimental study of vibratory gyroscopes or as a practical configuration for flight control and other applications.

The potential advantages of vibratory gyroscopes over conventional, rotating-wheel instruments are primarily low power consumption, long life and low manufacturing costs. It is obvious that if these advantages could be realized with instruments of suitable precision, the vibratory gyroscope would be preferred to conventional gyroscopes in many applications. Up to the present time, however, there have been very few if any, practical applications of vibratory gyroscopes. This is the result of the relatively low precision of the vibratory gyroscopes that have been developed up to the present time.

PRECISION LIMITATIONS

The observed low precision of vibratory gyroscopes does not appear to be associated with any fundamental barrier such as thermal noise. In fact, it has been shown that the thermal noise limit of vibratory gyroscopes is sufficiently low so that, if their precision were limited by it, these gyroscopes could detect angular rates of the order of 10^{-8}

[2] Electronic Systems Laboratory, Massachusetts Institute of Technology, Cambridge 39, Massachusetts

1* Superscript numerals in text refer to correspondingly numbered references at the end of this paper.

Unc.

radians per second (10^{-4} earth rate units, eru†).[2] Since the best tuning-fork gyroscopes that have been built so far are characterized by ten thousand times less precision than that determined by thermal fluctuations, it is evident that there must be other factors limiting the precision of these instruments.

Just as in the conventional gyroscope, the sources of error in the vibratory gyroscope are manifold. A number of these for the tuning-fork form of instrument have been pointed out by Morrow.[3] To date, one of the major barriers to high precision is associated with the forces required to drive the mass elements along their trajectories in the instrument frame of reference. Two types of forces are involved: those required to accelerate the mass elements and those required to overcome losses in the vibratory motion. In the ideal instrument these driving forces would not couple into the sensing system but in any actual instrument that has been so far devised small asymmetries and inhomogeneities cause minute fractions of the driving forces to couple into the sensing system. This unwanted cross coupling between the driving and sensing vibrations would not necessarily limit the precision of the instrument except for the fact that such coupling tends to vary in an erratic way with the passage of time and with changes in environmental parameters such as temperature and acceleration.

In order to understand more clearly how unwanted cross coupling can occur between the driven and sensed vibrations, we consider an idealized model for the double tuning fork used in the double modulation experiment. Figure 1 shows schematically the basic tuning fork structure. The arcuate motion of the opposed tines can be idealized as a straight line motion of two concentrated masses represented by the dotted spheres of Fig. 2. Ideally, these masses would move along the x_f axis. In practice, however, the paths of motion of the masses are not co-linear. To account for some of the affects of this departure from the ideal situation the line of motion of one mass can be regarded as displaced a distance ΔR on the positive side of the $x_f y_f$ plane and that of the other, on the negative side. Thus the masses in the non-ideal situation are represented by the solid spheres in Fig. 2. This displacement of the masses is termed torsional unbalance because it gives rise to the unwanted cross coupling between the driving and sensing vibrations. The displacement ΔR of the lines of motion of the masses of Fig. 2 corresponds to a form of mass unbalance in the actual tuning fork. But there are many other ways for cross coupling to be introduced and it is preferrable to think of this displacement as an equivalent representation of the numerous cross coupling effects.

The first step in an analysis of the model of Fig. 2 is to establish the Coriolis torque M_c that acts about the sensing axis y_f as the result of an angular rate of the tuning fork in inertial space. It will be recalled that the Coriolis force f_c apparently exerted by a moving mass m is given by

$$\vec{f}_c = 2m\,(\vec{v} \times \vec{\Omega}) \qquad (1)$$

where $\vec{v}$ is the velocity of the mass and $\vec{\Omega}$ is the angular rate of the frame of reference. Assuming simple harmonic motion for the mass, its displacement r from its rest position is given by

$$r = r_m \sin \omega_d t \qquad (2)$$

where r_m is the amplitude of motion and ω_d is the radian frequency of the driving vibration (which in practice is very close to the natural frequency of the tuning fork.)

† An earth rate unit, abbreviated eru, is 15 degrees per hour.

From Fig. 2 it is seen that the Coriolis torque about the sensing axis y_f is

$$M_c = -k_{Mc}\,\Omega_{yf}\cos\omega_d t \qquad (3)$$

where

$$k_{Mc} = 4m\,R\,r_m\,\omega_d \qquad (4)$$

Here the approximation has been made that the amplitude r_m of the movement of the mass is small compared to the rest radius R. The angular rate Ω_{yf} is the component of angular rate of the tuning fork that lies along the y_f axis. It is seen that the Coriolis torque about the sensing axis depends only on this rate and is independent of the rates about the other two fork axes. Also it should be noted that the Coriolis torque is a suppressed-carrier amplitude modulated representation of the input angular rate.

The next step in the analysis of Fig. 2 is to determine the cross-coupling torque M_{cc} about the sensitive axis y_f caused by the cross-coupling force f_{cc}. The cross-coupling force is the sum of the reaction force on the central member of the tuning fork required to balance the accelerating force of the mass m in its simple harmonic motion and the driving force needed to overcome losses. The accelerating force is supplied by the deflection of the tines represented by the bowing of the support line for the mass as shown in Fig. 2. From the model of Fig. 2 and the assumed simple harmonic motion for the driving vibration, the cross-coupling torque can be expressed as

$$M_{cc} = k_{Mc}\,\frac{\Delta R}{2R}\,\omega_d\left(\sin\omega_d t - \frac{1}{Q_d}\cos\omega_d t\right) \qquad (5)$$

where Q_d is the quality factor of the tuning fork in its driven mode. The first term in Eq. 5 is the reaction to the accelerating force and the second term accounts for the influence of the driving force needed to overcome losses. It is assumed that the driving means, not shown in Figs. 1 and 2, are external to the tuning fork structure. If these driving means were carried by the tuning fork structure the second term in Eq. 5 would not exist on the basis of the model of Fig. 2. However, because of asymmetries in loss paths between the fork and the instrument frame, it is to be expected that a loss term in the cross-coupling torque will appear even when the driving means are carried by the tuning fork structure.

The total torque M_s acting on the sensing axis is the sum of the Coriolis and cross-coupling torques, i.e., $M_s = M_c + M_{cc}$. On the basis of Eqs. 3 and 5 the total torque on the sensing axis can be expressed as

$$M_s = -k_{Mc}\left[(\Omega_{yf} - \Omega_d)\cos\omega_d t + \Omega_q \sin\omega_d t\right] \qquad (6)$$

where

$$\Omega_d \triangleq -\frac{\Delta R}{2R}\,\frac{\omega_d}{Q_d} \qquad (7)$$

$$\Omega_q \triangleq -\frac{\Delta R}{2R}\,\omega_d \qquad (8)$$

Ω_d is the equivalent rate representing the direct component of the cross-coupled signal and Ω_q is the equivalent rate for the quadrature component of the cross-coupled signal. If the cross-coupled components were constant they could be discriminated against by using

an appropriate phase angle for the reference of the demodulator that processes the signal derived from the vibration about the sensing axis resulting from the total torque M_s. Alternatively, these cross-coupled components could be cancelled by adding in appropriate signals prior to or following demodulation. It is the unfortunate fact, however, that the cross-coupled components do not remain constant but vary with time, temperature, acceleration and other influences. It is these variations in cross coupling that have limited the precision of vibratory gyroscopes that have been built so far. Thermal fluctuations are omitted in the above analysis because they are smaller than the cross-coupling variations by a factor of the order of 10^4 at the present state of the art.

DOUBLE MODULATION

Double modulation refers to the introduction of a second modulation of the Coriolis torque through modulation of the angular rates to be sensed. The first modulation is associated with the vibratory velocities of the masses imparted by the basic drive member, The additional modulation is introduced by rotating or oscillating the basic drive member about one of its rate insensitive axes. By way of example, Fig. 3 shows how a single-axis tuning fork instrument can be double modulated by rotation around its x_f axis at a constant angular rate ω_m. From Fig. 3 it is seen that the angular rate around the sensitive axis is given by

$$\Omega_{yf} = \Omega_y \cos \omega_m t + \Omega_z \sin \omega_m t \qquad (9)$$

where Ω_y is the angular rate around the y axis of the doubly modulated instrument and Ω_z is the corresponding rate around the z-axis.

In order to understand how double modulation affects the total torque around the sensing axis we first rewrite Eq. 7 as

$$M_s = -k_{Mc} \left[\Omega_{yf} \cos \omega_d t + \Omega_n (\cos \omega_d t + \theta_n) + \Omega_a \cos (\omega_d t + \theta_a) \right] \qquad (10)$$

In this equation the quadrature and direct components of the cross-coupling torque have been combined. This total cross-coupling is then separated into a non-acceleration sensitive component represented by the equivalent rate Ω_n at a phase angle θ_n and an acceleration component Ω_a at a phase angle θ_a (both functions of the acceleration vector). The non-acceleration dependent term is a slowly varying stochastic function of time and temperature (both the magnitude and phase angle vary). The acceleration dependent term arises primarily from unsymmetrical deflection of the tines under acceleration load. From Figs. 1 and 2 it is seen that the major contribution to the acceleration component will be caused by unequal deflection of the tines under the influence of acceleration a_{zf} along the z-axis of the fork. Thus we write approximately

$$\Omega_a \tilde{=} k_a a_{zf} \qquad (11)$$

where k_a is the first-order acceleration sensitivity. It is assumed for purposes of our preliminary analysis that the phase angle of the acceleration component of cross coupling is substantially constant. From Fig. 3 the acceleration along the z-axis of the fork under conditions of double modulation can be seen to be, ignoring possible steady centrifugal effects,

$$a_{zf} = - a_y \sin \omega_m t + a_z \cos \omega_m t \qquad (12)$$

where a_y and a_z are the accelerations along the y- and z-axis of the instrument. Placing the values for the angular rate given by Eq. 9 and the acceleration given by Eqs. 11 and 12

into Eq. 10 yields the following expression for the total torque about the sensing axis of the tuning fork.

$$M_s = M_{s+} + M_{sd} + M_{s-} \tag{13}$$

The three components, at frequencies $\omega_+ = \omega_d + \omega_m$ (upper sideband) ω_d (driving frequency), and $\omega_- = \omega_d - \omega_m$ (lower sideband), respectively, are:

$$M_{s+} \triangleq -\frac{k_{Mc}}{2}\left[(\Omega_y + k_a a'_y)\cos\omega_+ t + (\Omega_z + k_a a'_z)\sin\omega_+ t\right] \tag{14}$$

$$M_{sd} \triangleq -k_{Mc}\Omega_n \cos(\omega_d t + \theta_n) \tag{15}$$

$$M_{s-} \triangleq -\frac{k_{Mc}}{2}\left[(\Omega_y + k_a a''_y)\cos\omega_- t - (\Omega_z + k_a a''_z)\sin\omega_- t\right] \tag{16}$$

Here the primed and double primed accelerations refer to accelerations projected on axes rotated relative to the instrument axes in the positive direction about the x-axis. by angles of $\frac{\pi}{2} + \theta_a$ and $\frac{\pi}{2} - \theta_a$, respectively.

From Eqs. 13 through 16 the effect of double modulation, obtained through rotation of a single-axis instrument about one of its rate insensitive axes, is to produce torque components about the sensing axis at three frequencies instead of the single frequency that was present in the absence of double modulation. Equations 14 and 16 for the upper and lower sidebands, respectively, show that these torque components contain the desired rate information for rotation of the instrument around any line in the plane of the double-modulation spin. Equation 15 shows the existence of a non-doubly-modulated torque component at the tuning-fork driving frequency. This component is proportional to the non-acceleration-dependent cross-coupling represented by Ω_n. By suitable signal processing it is possible to have the overall instrument respond to either the upper or lower sideband to the exclusion of the other two components. In this way double modulation, at least theoretically, is able to discriminate between the desired rate signal and the undesired non-acceleration dependent cross-coupling in such a way as to exclude the latter. With respect to the acceleration-dependent cross-coupling, it is noted that the sideband torque components both contain terms that cannot be distinguished from the rate signals. Compensation for acceleration is possible to the extent that the coefficient k_a can be calibrated.

The above description of the double-modulation method of discriminating against non-acceleration dependent cross-coupling is a simplified discussion for the rotary method of double modulation that is valid only for small amplitudes of tine vibration and for negligible amplitude of torsional vibration of the fork about the sensing axis. More sophisticated analyses of the tuning-fork with rotary modulation, and of vibratory devices in general with double modulation introduced by oscillation rather than rotation, are given in the appendix.

To summarize, double modulation is the introduction of a modulation in addition to that associated with the oscillatory velocities of mass elements caused by the driving vibration. This additional modulation is for the purpose of discriminating against one major component of unwanted cross-coupling that in the past has severely limited the precision of vibratory gyroscopes. Torsional unbalance is a major contributor to this

component of cross-coupling. Analysis also shows that acceleration-dependent cross-coupling will not be discriminated against by double modulation and therefore will remain to be handled by other means in those situations where the acceleration error is too large. The question now arises: Does experiment confirm the theory of double modulation? The next two sections describe the experiments conducted to date and their results.

EXPERIMENTAL APPARATUS

A vibratory gyroscope that can be operated either with or without double modulation has been constructed so that the merits of double modulation can be evaluated experimentally. The goals of the experimental program are to compare the performances of the instrument in the two modes of operation and investigate the causes of zero rate drift with double modulation. The instrument is solely a laboratory model of convenient size to permit easy modification. It can be separated into three parts: the single-axis vibratory gyroscope or tuning fork unit, the double modulation carriage, and the signal processing electronics. Figure 4 shows the tuning fork unit installed in the carriage and Fig. 5 shows the tuning fork unit.

Tuning Fork Unit

The tuning fork unit is a single-axis vibratory gyroscope designed so that it can be rotated about an axis perpendicular to its rate-sensitive input axis. A double tuning fork is used as the drive member and a mechanical tuned system is used in the sensing mode. Tuning fork drive and a vibration detector electronic circuits are required for its operation as a single-axis vibratory gyroscope.

A double tuning fork, similar to that shown in Fig. 1, was selected because its symmetry simplified support problems when it is rotated and because it facilitates comparison with the considerable results of past research on tuning fork gyroscopes. Replaceable tines are used in the actual instrument to simplify machining and to reduce fatigue problems. Set screws are provided for rough balancing by changing the mass of the tines and moving the center of mass normal to the plane of vibration. The double modulation rotation axis is perpendicular to the fork input axis y_f and coincides with the x_f axis when the fork is inertially stationary. The adjacent tines of the two tuning forks are coupled together by small springs and are magnetically driven. The amplitude and frequency of the fork vibration are maintained constant by the tuning fork drive circuit that has as its input a signal from reluctance type pickups sensing the motion of the tuning fork tines and as its output the coils of the magnetic drivers.

As shown in the preceeding section, when angular rates are applied to the unit about the y_f axis, torques proportional to the product of these rates and the sinusoidal velocity of the tuning fork tines are impressed on the tuning fork about the y_f axis. The resulting twisting motion of the tuning fork with respect to the case is usually sensed to provide the electrical output. This motion can be maximized by making the torsional resonant frequency of the fork and suspension about the y_f axis equal to the carrier frequency of the torques. Resonant sensing lowers the instrument threshold; however, the resulting twisting of the fork through large angles is undesirable because it increases the interaxis cross-coupling of rates from the x_f axis and decreases the useful dynamic range of the instrument. In order to alleviate these difficulties while still maintaining the beneficial characteristics of resonant sensing, a counterpoise sensing scheme is used in this instrument. The counterpoise is an inertia much smaller than the tuning fork inertia which is attached to the tuning fork by means of a torsion bar along the y_f axis. If the system is properly designed, the counterpoise and tuning fork vibrate in phase opposition and the amplitude of the counterpoise is much larger than that of the fork when torques are applied to the tuning fork at the upper resonant frequency of the combination. Higher Q's (quality factor) are achievable with this scheme than with the single tuned system and the undesirable motion of the drive member is greatly reduced.

The counterpoise element, shown in Fig. 1, is attached to the torsion rod which is along the y_f axis of the tuning fork. It is in the form of a plate which together with insulated plates attached to the tuning fork center piece forms a differential capacitor. This capacitor is in a capacitance bridge which is excited at a low radio frequency from the vibration detector circuit. The bridge output is then amplified, rectified and filtered to provide an electrical signal proportional to the angle between the tuning fork and counterpoise.

The torsion rod is attached to the tuning fork by collets at the ends of the fork and the ends, together with four spokes attached to each end of the fork, provide support for the tuning fork with respect to the case. The fork is therefore rigidly supported in all modes except the torsional mode about the y_f axis.

The upper resonant frequency of this suspension has been tuned to the lower sideband of the torques which are applied to the tuning fork when the unit is double modulated. These torques occur at the tuning fork frequency minus the double modulation frequency. The large magnitude and wide band characteristics of the noise torques applied to the tuning fork justify discarding the energy in one sideband in order to achieve better filtering. When this instrument is operated without double modulation, however, it is off resonance. Since the noise torques in the non-double modulated instrument are at the same frequencies as the signal and we are well above the threshold of the detector, the performance is not degraded. Therefore, it is possible to use the same tuning fork unit for the comparison tests.

Double Modulation Carriage

The double modulation carriage rotates the tuning fork unit and associated electronics about an axis that can be oriented at any angle with respect to vertical. The carriage is turned by a printed circuit motor driven by silicon controlled rectifiers and is phase locked to a stable low frequency oscillator. Tapered roller bearings were used in the initial tests and other types are being investigated.

Accurate control of the carriage speed is necessitated by the high Q mechanical resonance in the sensing mode of the tuning fork unit. It is accomplished by sampling the output of a stable, low-frequency oscillator twice each revolution of the carriage and using this error signal to control the firing angle of the SCR's driving the motor. The sampling occurs when two diametrically opposed slots in a disc rotating with the carriage pass a light source and allow the light to reach a photodiode.

Signal Processing Electronics

Figure 6 shows a block diagram of all the electronic circuits used in the experiment. The signal processing electronics consist of two ring demodulators, one phase shifter and several linear amplifiers and filters. The vibration detector, tuning fork drive and speed control have been discussed in the sections on the tuning fork unit and the double modulation carriage.

The signal from the vibration detector, which is proportional to the angle between the counterpoise and tuning fork, is first demodulated using as the reference a phase-shifted signal from the tuning fork drive. When the instrument is operated without double modulation the output of the demodulator is passed through a low pass filter to obtain a d-c signal proportional to the applied rate. The transfer function for the instrument relating the input rate and the output voltage has the frequency characteristics of the low-pass filter.

When the instrument is operated with double modulation the output of the first demodulator is transmitted through a band-pass filter centered at the double-modulation

frequency. This signal is then demodulated using as the reference a square wave phase locked to the carriage. The output of the demodulator is passed through a low pass filter to obtain a d-c signal proportional to the applied rate about either the y or z axes depending on the phase of the reference of the second demodulator. The transfer function relating the input rate and output voltage now depends on the quality factor Q_s of the mechanical sensing system, the band-pass filter following the first demodulator, and the low-pass filter following the second demodulator. The band-pass filter characteristics can be neglected since the filter is needed only to separate the signal from d-c and the second harmonic of the tuning fork frequency. For data transmission, the mechanical resonance contributes a first order pole with a time constant expressed by

$$\tau = \frac{2Q_s}{\omega_s} \qquad (17)$$

where

Q_s = quality factor at frequency ω_s

ω_s = upper resonant frequency of the suspension

EXPERIMENTAL DATA

The tuning fork gyroscope described above has been successfully operated with and without double modulation. Although double modulation greatly improved the performance of the instrument, the data presently available are not sufficient to draw final quantitative conclusions. Research is continuing on the instrument so that a better understanding of the performance limitations can be obtained

TABLE 1 INSTRUMENT PARAMETERS

Parameter			Value		
Tuning Fork Frequency	-	$\frac{\omega_d}{2\pi}$	358.6	cps	(ω_m=0)
Upper Resonant Frequency	-	$\frac{\omega_s}{2\pi}$	312	cps	(ω_m=0)
Lower Resonant Frequency	-	$\frac{\omega_l}{2\pi}$	31	cps	(ω_m=0)
Double Modulation Frequency	-	$\frac{\omega_m}{2\pi}$	45.19	cps	
Tuning Fork Constant Inertia	-	Iyo	1000	gm cm^2	(approximate)
Ratio of Modulated Tuning Fork Inertia to Unmodulated	-	α_y	.03		(approximate)
Quality Factor Associated with the Upper Resonant Frequency ω_s	-	Q_s	580		
Bandwidth of Electrical Filtering	-	BW	0.5	cps	

Figures 7 and 8 show typical output recordings from the instrument. In both modes of operation the instrument was in free air and no attempt was made to control the temperature. Non-resonant double modulation data have been omitted because they are inferior to the resonant data.

Table 2 shows the performance characteristics of the instrument for both modes of operation. These numbers have been taken from the data shown in the six traces of Figs. 7 and 8 and are representative of the instrument performance as of September 1963; however, they are not final data since research is continuing on the instrument. The drift characteristics of the zero-rate signals have been separated into long and short term values. Short term is defined as one minute and long term, twenty minutes, the maximum recording time used so far. By considering the various drift mechanisms, however, some conclusions can be drawn from the data.

TABLE 2 PERFORMANCE CHARACTERISTICS

Parameter	Without Double Modulation		With Double Modulation
Standard Deviation of Short Term Drift	6	eru	6 eru
Standard Deviation of Long Term Drift	44	eru	Not Observable
Magnitude of Zero-Rate Signal	5650	eru	60 eru
Phase Shift Sensitivity	100	$\frac{\text{eru}}{\text{degree}}$	1 $\frac{\text{eru}}{\text{degree}}$

The short term noise characteristics are different in the two modes of operation because of the large amount of noise contributed by the bearings. When the output of the vibration detector was viewed on an oscilloscope, while the carriage was turning, narrow band noise at the frequency ω_s obscured the tuning fork frequency unbalance signal and did not change noticeably when the tuning fork was turned off. Nevertheless the instrument short term drift performance was unchanged when double modulation was applied. If the source of the 0.8 cps noise component visible on the traces of Fig. 8 was known and removed, the short term performance would even be better by approximately a factor of 3 with double modulation. In either mode of operation the short term characteristics would not have changed if the temperature had been controlled because the main sources of noise without double modulation are the random tuning fork unbalance and electronic noise whereas with double modulation it is the bearings. Better tuning fork balance would reduce the noise due to drift in the demodulator electronics by decreasing the quadrature signal, however the random balance and associated drift should remain about the same. Therefore the limiting factors determining short term drift characteristics are the relatively crude tuning fork and bearings used in the experiment. The short term noise in both modes of operation could probably be reduced by two orders of magnitude in a more sophisticated instrument. However, it is felt that the present instrument and data are partial to neither mode of operation and the relative short term performances are characteristic of double modulated vibratory gyroscopes.

Long term drift was greatly improved when double modulation was employed. Much of the drift without double modulation is thought to be attributed to temperature-balance effects in the tuning fork since the frequency of the tuning fork was observed to decrease with time indicating the fork temperature was increasing. The temperature coefficient for the tuning fork is approximately 0.06 $\frac{\text{cps}}{^{o}\text{C}}$. This does not mean that controlling the temperature of the tuning forks would eliminate the long term drift without double modulation, however, because material creep and electronic drift become important as other tuning fork instruments have demonstrated. The effect of electronic drift in the demodulator is directly proportional to the magnitude of the zero-rate signal which was reduced from 5650 eru without double modulation to 20*eru with double modulation. A further reduction is expected with double modulation when acoustic reflection problems are eliminated. Material creep is only a problem without double modulation and has not been investigated.

Lack of temperature control may appear to be a means of deliberately biasing the results in favor of double modulation, however, longer time traces should also show the merits of double modulation in this instrument temperature controlled to within 0.1°C.

* Of 60 eru observed 40 eru was due to acceleration of gravity. This was in phase with the rate signal and equal to the predicted value.

Furt... ...e temperature control is a power consuming luxury which may be eliminated through double modulation. Without double modulation the drift is a function of the balance of the tuning fork which varies with temperature and requires hours to reach equilibrium in a constant temperature environment. With double modulation the long settling time associated with the fork balance is no longer a problem and temperature drift is a function of the change in the difference between the drive and output resonant frequencies. Since these are both mechanical resonances and the materials are at the same temperature, the effect can be made second order. Warm up time may therefore be reduced from hours to seconds by double modulation.

Additional data are being taken on the instrument to obtain a more complete comparison of the performances with and without double modulation. It is evident from the present data, however, that double modulation should improve the present instrument long term drift performance by at least a factor of 100,

CONCLUSIONS

1. Major source of imprecision in vibratory gyros has been unwanted cross-coupling between driving and sensing modes.

2. In tuning-fork devices torsional unbalance is a major source of cross-coupling.

3. Double modulation theoretically discriminates against all non-acceleration dependent unwanted cross-coupling.

4. Experimental tests of a vibratory gyroscope without accurate temperature control using a tuning-fork configuration with and without rotary double modulation have shown:

   a. Improvement in zero-rate error attributed to non-acceleration dependent cross-coupling of at least a factor of 100 has been achieved by double modulation. This result has been obtained in spite of a high level of double modulation bearing noise that tends to bias the result in favor of the test without double modulation. The single axis tuning-fork device used in the above experiments is characterized by a torsional unbalance that is larger than the unbalance of the best tuning-fork gyroscopes by a factor of 500.

   b. Zero-rate error attributed to acceleration dependent cross-coupling is not affected by double modulation.

   c. Double modulation spin axis bearings do not appear to be critical.

5. An extrapolation of the above results would indicate that double modulation applied to the best tuning-fork instruments would yield zero-rate uncertainty of the order of 10^{-2} eru or less.

6. For long life, low power, space applications an all vibratory system offers advantages if performance similar to that forecast for rotary double modulation can be obtained.

7. Temperature control may not be necessary with double modulation and warm up times may be reduced from hours to seconds.

ACKNOWLEDGEMENT

The above study of double modulation in vibratory gyroscopes was conducted in the Electronic Systems Laboratory, Electrical Engineering Department, Massachusetts Institute of Technology under support extended by the National Aeronautics and Space Administration, Office of Research Grants and Contracts (Grant No. NSG-149-61). The opinions and conclusions reflect the views of the authors and are not recommendations or conclusions of the sponsor.

APPENDIX A

DOUBLE MODULATION BY VIBRATION

Double modulation can be accomplished by either a vibration or a rotation about one or more axes. When rotary double modulation about one axis is used the frequencies of the torques containing the rate information are the drive frequency plus and minus the double modulation frequency. When vibratory double modulation about one axis is employed these torques occur at the drive frequency plus and minus odd harmonics of the double modulation frequency. This can be seen by examining the rates appearing along the input axis of the tuning fork example shown in Fig. 3 if we make

$$\theta = \theta_o \cos \omega_m t \tag{A-1}$$

$$\Omega_{yf} = \sum_{n=\infty}^{\infty} \left[\Omega_y J_n\left(\frac{\theta_o}{2}\right) \cos n\, \omega_m t - \Omega_x J_n \left(\frac{\theta_o}{2}\right) \sin n\, \omega_m t \right] \tag{A-2}$$

where J_n is a Bessel Function of order n.

APPENDIX B

THEORY OF OPERATION OF TUNING FORK GYROSCOPE EMPLOYING DOUBLE MODULATION

Two differential equations (Eqs. B-1 and B-2) describe the ideal double modulated tuning fork gyroscope when inertial rates are applied about the y and x axes shown in Fig. 9. Terms involving rates about the z axis are omitted because of their similarity to y axis terms.

$$\begin{aligned} &I_y(1+a_y \sin\omega_d t)\ddot{\theta}_1 + (f_1+f_2+a_y I_y \omega_d \cos\omega_d t)\dot{\theta}_1 + \{K_1+K_2+[Ix-Iz(1+a_z \sin\omega_m t)]\omega_m^2\}\,\theta_1 \\ &= f_2\dot{\theta}_2 + K_2\theta_2 + I_y(1+a_y \sin\omega_d t)\left[\Omega_y \omega_m \sin\omega_m t - \dot{\Omega}_y \cos\omega_m t\right] \\ &\quad - I_y a_y \omega_d \cos\omega_d t\left[\Omega_y \cos\omega_m t\right] \\ &\quad + \left[I_z(1+a_z \sin\omega_d t) - I_x\right]\left[\Omega_x^2\theta_1 + \Omega_y^2\theta_1 \sin^2\omega_m t - \Omega_y(\omega_m+\Omega_x)\sin\omega_m t\right] \end{aligned} \tag{B-1}$$

$$\begin{aligned} &Iy_c\ddot{\theta}_2 + f_2\dot{\theta}_2 + \left[K_2+(Ix_c-Iz_c)\omega_m^2\right]\theta_2 = f_2\dot{\theta}_1 + K_2\theta_1 + Iy_c\left[\Omega_y\omega_m \sin\omega_m t - \dot{\Omega}_y \cos\omega_m t\right] \\ &\quad + \left[Iz_c - Ix_c\right]\left[\Omega_x^2\theta_2 + \Omega_y^2\theta_2 \sin^2\omega_m t - \Omega_y(\omega_m+\Omega_x)\sin\omega_m t\right] \end{aligned} \tag{B-2}$$

where

I_x = Moment of inertia of the tuning fork about the x_f axis

$I_y(1+a_y \sin\omega_d t)$ = Moment of inertia of the tuning fork about the y_f axis

$I_z(1+a_z \sin\omega_d t)$ = Moment of inertia of the tuning fork about the z_f axis

Ix_c = Moment of inertia of the counterpoise about the y_c axis

Iy_c = Moment of inertia of the counterpoise about the y_c axis

Iz_c = Moment of inertia of the counterpoise about the z_c axis

K_1 = Spring constant for torsion rod and spokes supporting the tuning fork

K_2 = Spring constant for torsion rod between tuning fork and counterpoise

f_1 = Loss term associated with K_1 spring

f_2 = Loss term associated with K_2 spring

Ω_y = Inertial rate applied about the y axis

Ω_x = Inertial rate applied about the x axis

θ_1 = Angle between the tuning fork and the case

θ_2 = Angle between the counterpoise and the case

ω_m = Double modulation frequency

ω_d = Tuning fork or drive frequency

The differential equations were derived using Lagranges method and making the following assumptions.

1. Higher harmonic terms of the tuning fork inertias are small and are dropped

2. Double modulation motion is planar

3. The tuning fork and counterpoise are rigidly constrained except in the torsional mode about the y_f axis.

The last term of Eq. 2 can be eliminated by making $Ix_c = Iz_c$. The remaining time-varying term represents a torque applied to the counterpoise member at the double modulation frequency. Since we are using resonant sensing and synchronous demodulation this term can be neglected and the resulting equation shows that the counterpoise element acts in the intended manner as a vibration damper. The last term of Eq. 1 contains the interaxis cross-coupling terms and second order terms in the applied rates. From these terms performance limitations of the instrument can be determined. Even when all these terms are dropped, the time varying coefficients make it difficult to solve the equations exactly. An approximate solution can be obtained by using the average values of the coefficients. A more exact solution can be obtained by using properties of Mathieus[4] equation.

In the following analysis the simplified theory is used to determine the approximate behavior of the instrument. Forcing functions at the double modulation frequency, interaxis cross coupling terms and second order terms have been dropped. F(t) is the forcing function at the two sidebands ($\omega_d \pm \omega_m$) and is expressed by

$$F(t) = \frac{1}{2} I_y a_y \omega_d \left[\left(1+\beta \frac{\omega_m}{\omega_d}\right) \cos (\omega_d - \omega_m)t + \left(1-\beta \frac{\omega_m}{\omega_d}\right) \cos (\omega_d + \omega_m)t \right] \qquad \text{(B-3)}$$

where β is a function of the inertia of the tuning fork.

$$Iy\ddot{\theta}_1 + (f_1+f_2)\dot{\theta}_1 + [K_1+K_2+(Ix-Iz)\omega^2_m]\,\theta_1 = f_2\,\dot{\theta}_2 + K_2\dot{\theta}_2 - F(t) \qquad \text{(B-4)}$$

$$Iy_c\ddot{\theta}_2 + f_2\dot{\theta}_2 + K_2\theta_2 = f_2\dot{\theta}_1 + K_2\theta_1 \qquad \text{(B-5)}$$

Since the equations are linear, the following transfer function relating the output angle $(\theta_2-\theta_1)$ to the forcing function $F(t)$ can be obtained.

$$\frac{\theta_2(s)-\theta_1(s)}{F(s)} = \frac{s^2}{Iy(s^2+\frac{\omega_l}{Q_l}s+\omega_l{}^2)(s^2+\frac{\omega_s}{Q_s}s+\omega_s{}^2)} \qquad \text{(B-6)}$$

where

ω_l = lower resonant frequency

ω_s = upper resonant frequency

Q_l = quality factor associated with the lower resonant frequency

Q_s = quality factor associated with the upper resonant frequency

If ω_m is made equal to the drive frequency minus the upper resonant frequency of the mechanical system and $\omega_l \ll \omega_s$, the envelope transfer function for lower sideband of $F(t)$ is expressed by Eq. 7

$$\frac{[\,\theta_2(s) - \theta_1(s)\,]_E}{\Omega y\ (s)} = \frac{a_y\,\omega_d(1+\beta\,\frac{\omega_m}{\omega_d})\tau}{4\omega_s\,(\tau s+1)} \qquad \text{(B-7)}$$

The upper sideband is separated from the resonant frequency by $2\omega_m$ and the cross-coupled tuning fork drive signal by ω_m so they are attenuated with respect to the lower sideband from which we are extracting the rate information.

If we drop the term $\beta\,\frac{\omega_m}{\omega_d}$ and make the approximation $\omega_m \cong \omega_d$, the approximate sensitivity of the mechanical parts of the instrument, defined as the ratio of the input angular rate to the output vibration angle for constant input rates, is expressed by Eq. B-8.

$$K_m = \frac{a_y\tau}{4}\ \text{sec} \qquad \text{(B-8)}$$

Therefore the approximate gain bandwidth product for the mechanical components is $\frac{a_y}{4}$ or simply a function of the ratio of the modulated to unmodulated inertias of the drive member. This is a useful figure of merit for vibratory gyroscopes and can be increased in a given configuration by decreasing the drive frequency since material strain is the limiting factor.

REFERENCES

1. Lyman, J., "New Space Rate Sensing Instrument", Aeronautical Engineering Review, 12, 24-30 (1953)

2. Newton, G.C. Jr., "Comparison of Vibratory and Rotating-Wheel Gyroscopic Rate Indicators", AIEE Trans., Pt. II, 79, 143-150 (1960)

3. Morrow, C.T., "Zero Signals in Sperry Tuning Fork Gyrotron", J. Acoustical Society of America, 27, 581-85 (1955)

4. Fearnside, K. and P.A.N. Briggs, "The Mathematical Theory of Vibrating Angular Tachometers", Proc. I.E.E. 105 (Pt. C) 155-166 (1958)

ABSTRACT

Vibratory drive, vibratory output instruments for sensing angular rates, such as tuning forks, potentially offer certain advantages over conventional gyroscopes. The theoretical performance of these devices has not been realized experimentally because of zero-rate errors attributed to mass unbalance, driving force unbalance and other imperfections. By separating the driving and sensing frequencies through a process called double modulation, obtained through an additional rotation or vibration of the basic sensing element, zero rate errors may be diminished. Theoretical and experimental evidence in support of the double modulation concept is presented. A tuning fork type of instrument has been used in the initial experiments and a substantial improvement over the performance of the same instrument without double modulation has been realized.

LIST OF CAPTIONS

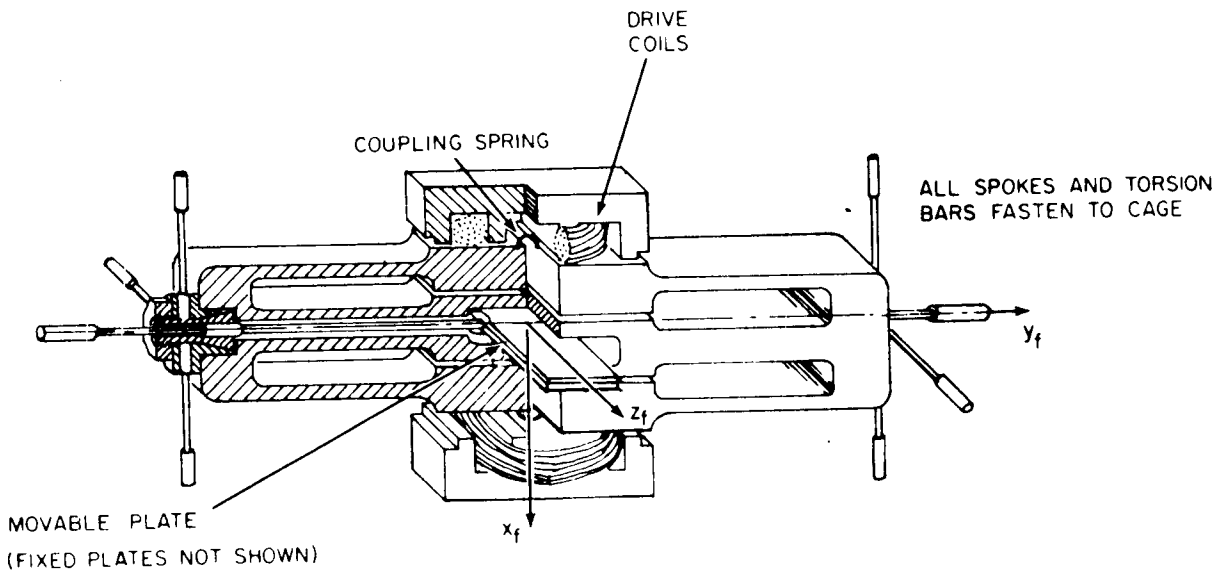
DRIVE
COILS
COUPLING SPRING
ALL SPOKES AND TORSION
BARS FASTEN TO CAGE
y_f
z_f
x_f
MOVABLE PLATE
(FIXED PLATES NOT SHOWN)

Fig. 1

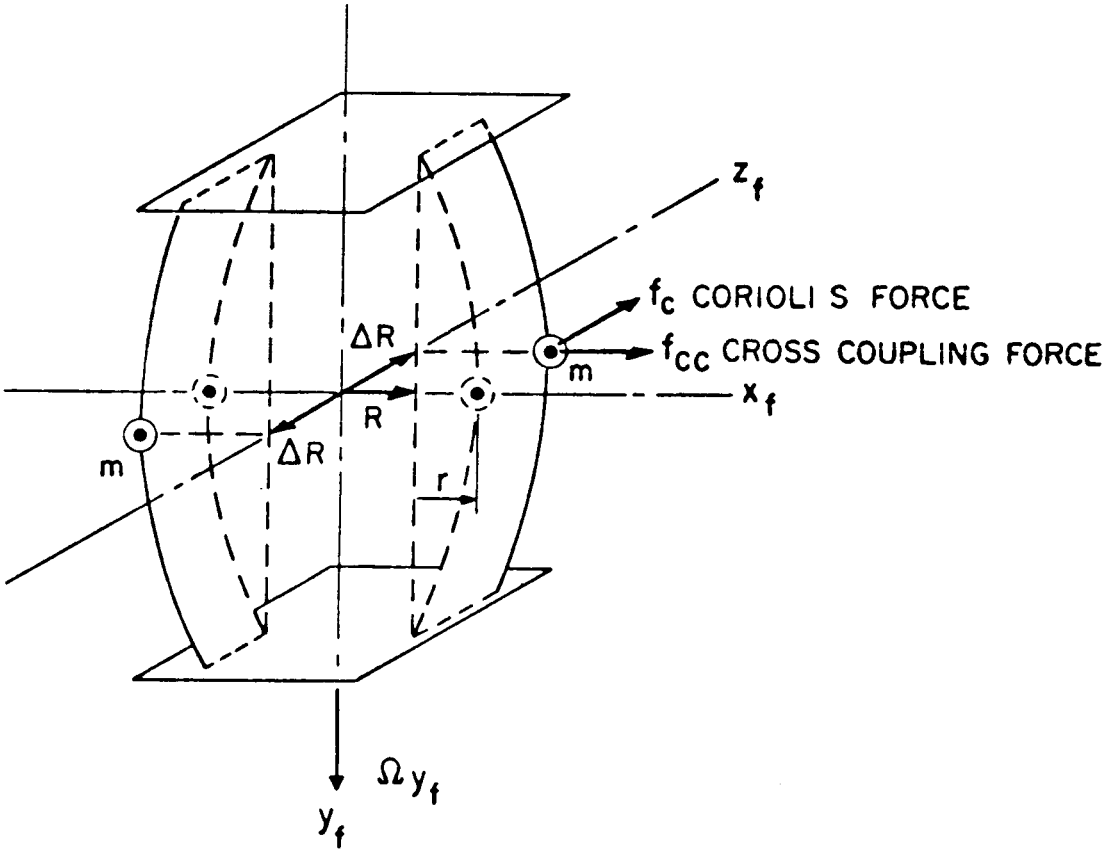

FIG. 2

BUSH-NEWTON

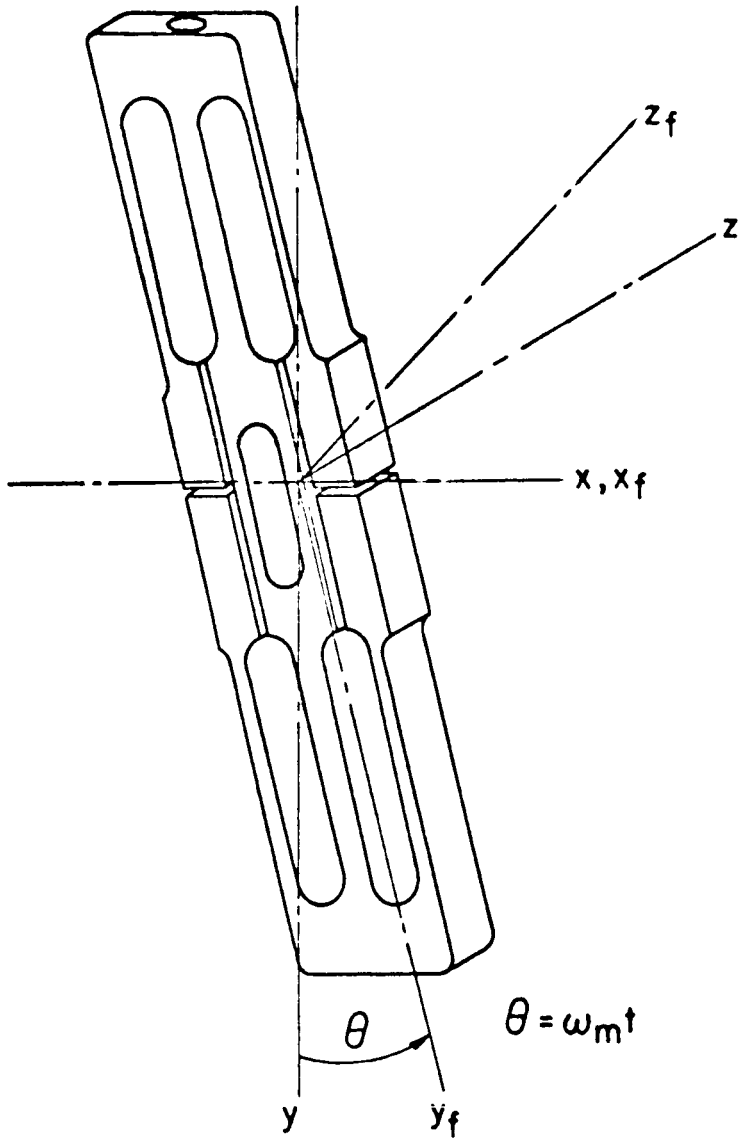

FIG. 3

BUSH-NEWTON

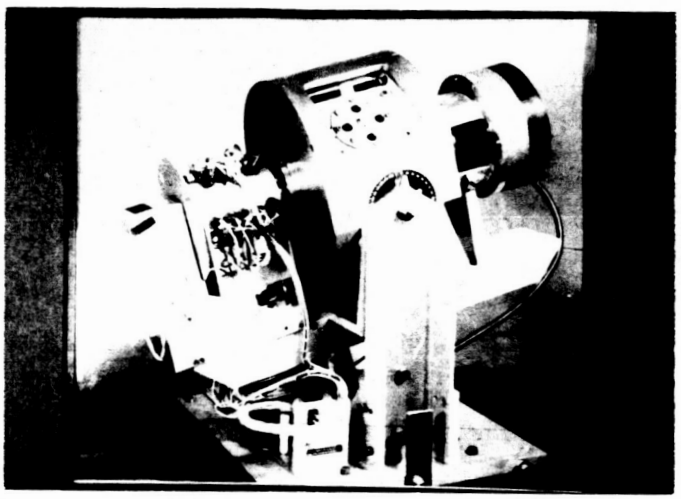

FIG. 4

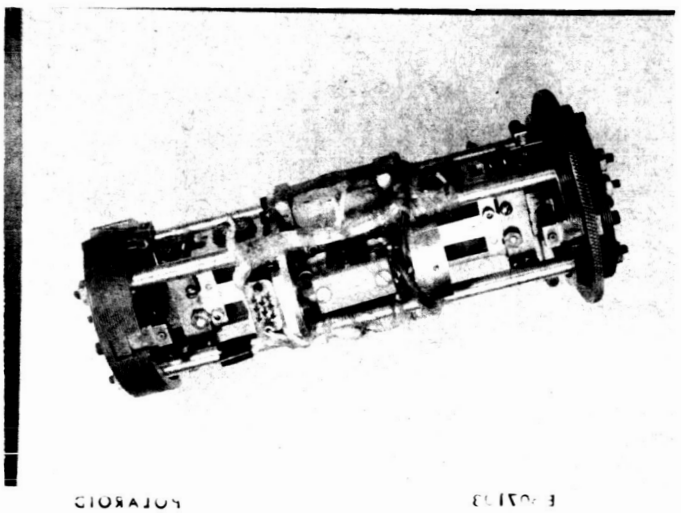

FIG. 5

TOP

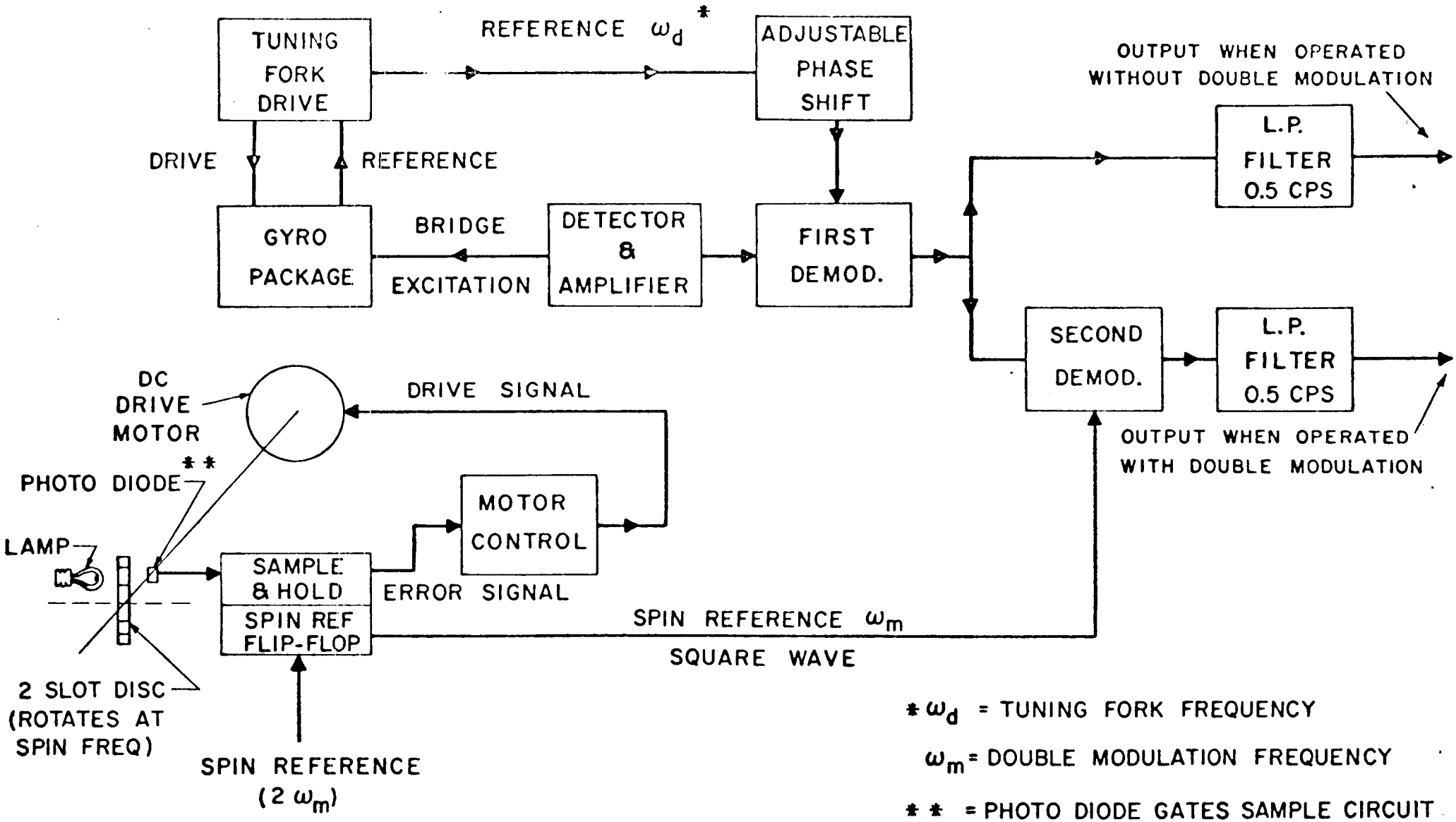

* ω_d = TUNING FORK FREQUENCY

ω_m = DOUBLE MODULATION FREQUENCY

** = PHOTO DIODE GATES SAMPLE CIRCUIT & SPIN REFERENCE FLIP-FLOP

FIG. 6
BUSH - NEWTON

R.W. BUSH 16 JULY 63
OUTPUT OF FIRST DEMOD
D.M. SPEED 0
INPUT SIGNAL 1.2 V P to P
SANBORN SENSITIVITY x 1

TUNING FORK FREQ 358.71
BEARINGS - TAPERED ROLLER
ADJUSTED - TIGHT

5 mu CALIB

-88 cru

-22 cru

+22 cru

f_{tf} 358.70

INPUT SIGNAL INCREASED TO 1RV P to P

+11 cru

-11 cru

0

f_{tf} 358.71

R.W. BUSH 16 JULY 63°
SAME AS ABOVE
LONG TERM ZERO RATE DRIFT
SANBORN SENSITIVITY x1
INPUT SIGNAL 1.2 V P to P.

tuning fork freq monitored

f_{tf} 358.68

f_{tf} 358.67

R.W. BUSH 16 JULY 63
OUTPUT OF FIRST DEMOD f_{dm} = 0
SANBORN SENSITIVITY x 20
PHASE SHIFT DATA

INPUT SIGNAL (QUADRATURES)
1.2V P to P

R = ALL RATES 32x88 cru

QUADRATURE 2% 6650 cru.

5mu CALIB

-1.8°
-3.6°
-4.4°
-7.2°
-9.0°

+1.8
+3.6°
+4.4°
+7.2°
+9.0°

PHASE SHIFTS OBSERVED ON SCOPE

SANBORN SENSITIVITY CHANGED TO x 100

+R
-R
45° SHIFT
+R
-R
+R
45° SHIFT

FIG. 7
BUSH-NEWTON

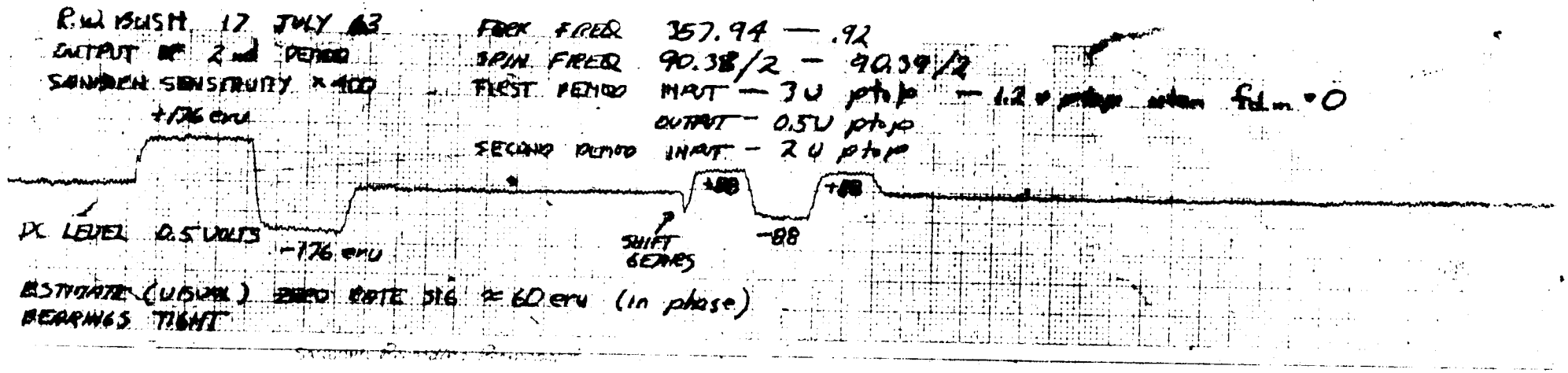

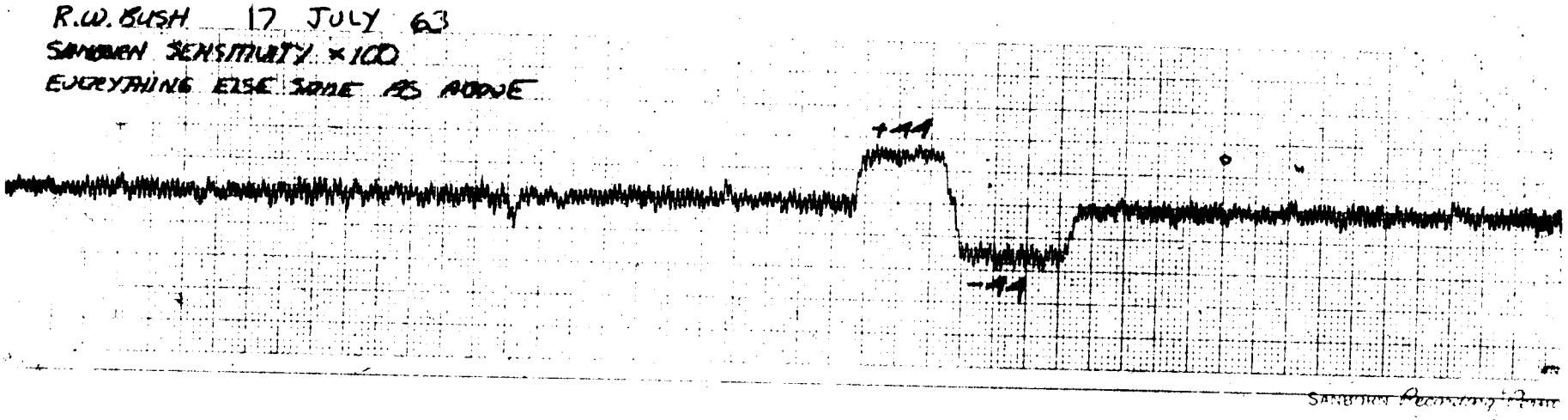

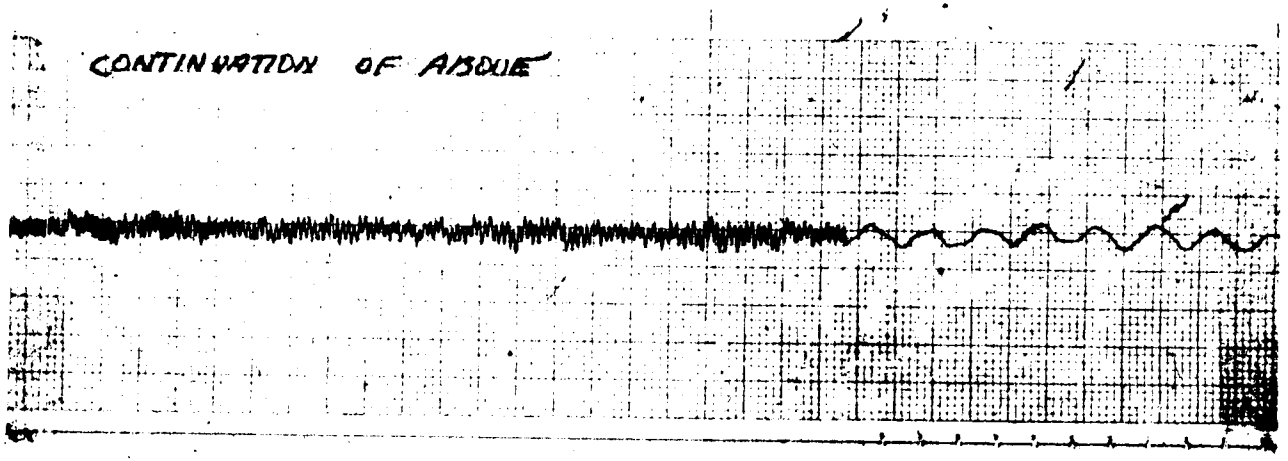

FIG. 8
BUSH-NEWTON

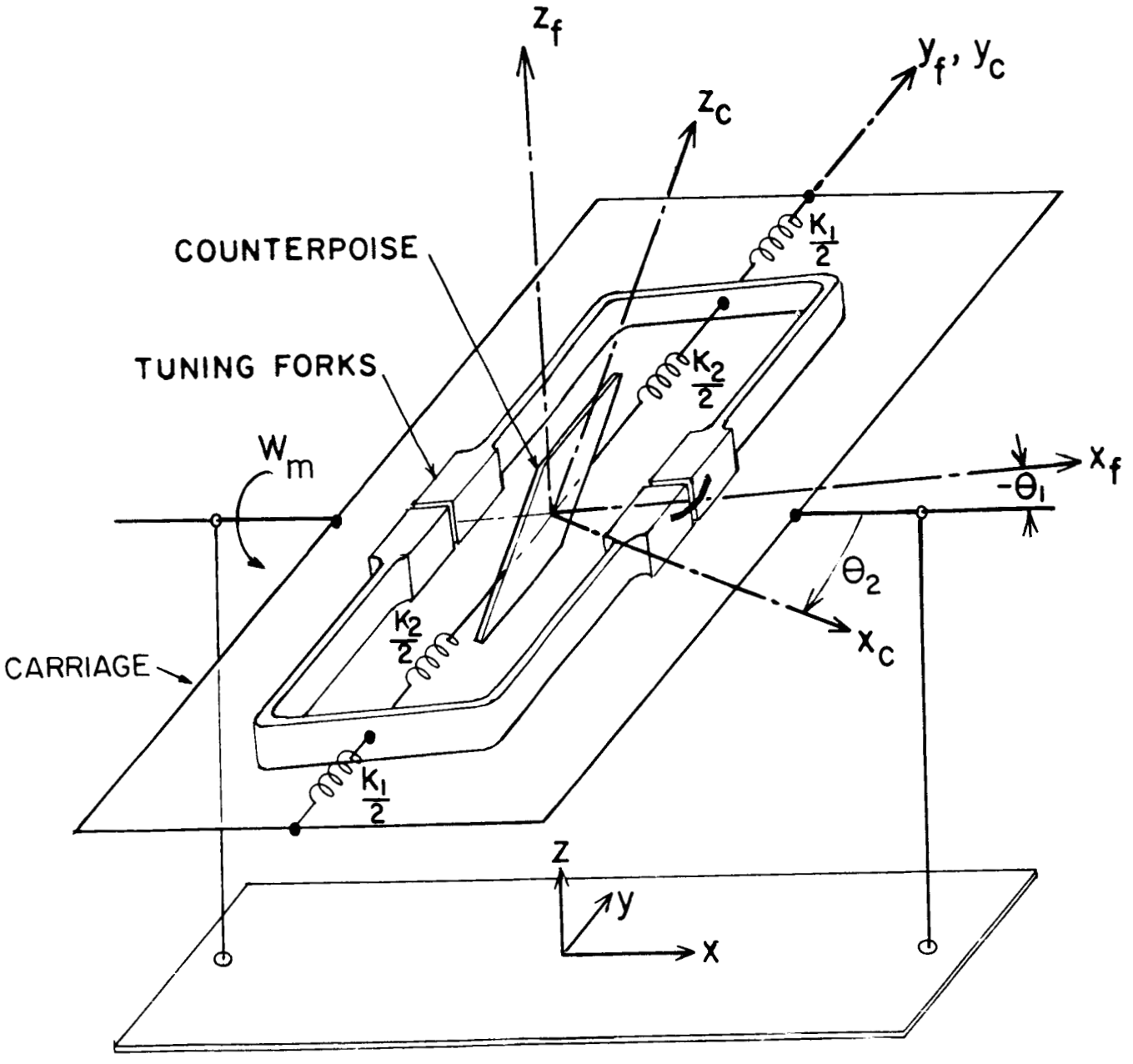

FIG. 9

BUSH - NEWTON